Discussions on the influence of residual stresses to the fatigue of layered polymer composites

Ilja Koch, Gordon Just, Maik Gude
Institute of Lightweight Engineering and Polymer Technology - ILK, Department of mechanical engineering, Technische Universität Dresden, Holbeinstr. 3, 01307 Dresden, Germany

e-mail: ilja.koch@tu-dresden.de; gordon.just@tu-dresden.de; maik.gude@tu-dresden.de

Ilja Koch is head of the group of testing methods and experiments at Institute of Lightweight Engineering and Polymer Technology of TU Dresden. He is working in the area of fatigue of composite materials both experimentally and analytically since 2004.

Gordon Just is member of the scientific staff at Institute of Lightweight Engineering and Polymer Technology since 2013. He is working in the area of damage and fatigue analysis and modelling of composite materials. Current investigations aim at the influence of load ratio.

Abstract

The fatigue behaviour of multi-layered fibre reinforced composites is under investigation since many years. In the recent years the scale of describing fatigue damage is shifting from the macroscopic to the mesoscopic scale. On that background a research project has been set up to analyse and mathematically describe specifically the influence of reversed cyclic loading to the damage and failure behaviour of composites. At ILK therefore the global stress-strain behaviour during tension and compression loading is correlated with the local (layerwise) deformation behaviour. It is shown by digital image processing of microscopic images that residual tension stresses in off-axis plies lead to significant residual crack opening. From DIC-measurements of cracked laminates on the mesoscale at tension and compression loading it is proven, that opened cracks are gradually closed during compression, leading to nonlinear stress-strain behaviour. Regarding layerwise damage

analysis it is therefore a necessity to consider manufacturing induced residual stresses which lead to significant differences in the local stress ratio compared to the macroscopic loading.

1 Introduction

The work presented here is part of a collaborative project of Polymer Composites (TU Hamburg-Harburg), IKV (RWTH Aachen), ILK (TU Dresden) and ISD (Leibniz Universität Hannover) funded by the German Research Foundation (DFG). It focusses the analysis of multi-scale damage of endless fibre reinforced composites under reversed cyclic loading.

At ILK (TU Dresden) the analytical and experimental work is currently focussed on the understanding and description of transverse cracking in cross-ply laminates at different stress ratios including manufacturing induced residual stresses.

Residual stresses not only lead to deviations of the shape of complex structures after fabrication [1] but also influence the damage and failure behaviour to a wide extend. For the case of multi-layered hot hardening epoxy matrix and carbon fibre reinforced systems, which are in focus here, residual stresses on different length scales develop during curing and tempering cycles. On the scale of fibre and matrix the development of residual stresses is driven by the difference of thermal and chemical shrinking of fibre and matrix. On the scale of the unidirectional layer comparable effects yield residual stresses, but here due to anisotropic shrinking of the unidirectional layer. Besides the mechanical and thermal properties of fibre and matrix as well as the fibre volume fraction, the layer thickness and stacking sequence influence the amount and the distribution of the layerwise remaining stress field [2]. In case of viscoelastic or viscoplastic deformations also the exposure time and temperature are relevant.

The time dependent local stress field, which is driving the initiation and growth of cracks and failure, is a superposition of local remaining stress field and macroscopic static and cyclic loading. The residual stresses do not alternate and therefore contribute only to the mean stress. The local stress ratio, which is a main parameter to be considered in durability analysis, deviates from the macroscopic load ratio. It is therefore mandatory to consider residual stresses for quantifying strength values and fracture energies in mechanical tests and virtual material characterisation approaches [2].

After short remarks to material, experimental methods and residual stresses, their influence on local fatigue stresses are discussed in more detail.

2 Materials and specimen preparation

The investigations on the crack opening displacement are performed on cross-ply laminates comprised of carbon T700SC 6k fibre rovings provided by TORAY INTERNATIONAL INC. and ARADLITE LY556 epoxy resin system. First, the lay-up is built by a dry winding process on to a specific winding core providing two stacks at a time. Afterwards, the resin transfer moulding is used to infiltrate the dry preform with the resin system. The laminates are cured at 80 °C for 3 hours and post-cured at 150 °C for 4 hours and have an approximate fibre volume fraction of 60 %. Aluminium end tabs with a thickness of 2 mm are applied to the fibre reinforced plate using epoxy based glue SCOTCH WELD DP-490. The specimens are cut to size from the assembled plate with a high precision abrasive-cutting machine and have a total length of $L = 190$ mm, width $W = 25$ mm and a laminate thickness of $H = 2$ mm. Specimen dimensions and the lay-up are given in figure 1.

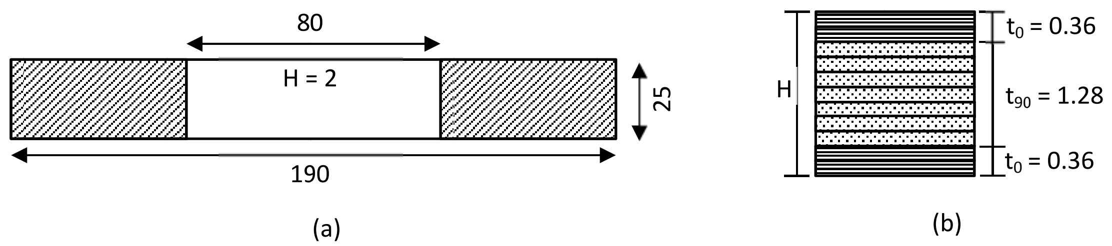

Figure 1: **Dimensions (a) and lay-up (b) of the specimens used in fatigue testing and COD-analysis. All dimensions are given in millimetres (mm).**

As one aim of the investigation is the detailed analysis of the transverse cracks, the specimen edges are polished up to a grain size of 5 µm, ensuring a clear view and high contrast between fibres and matrix.

The elastic and strength properties of the composite material are determined by testing of unidirectional specimens in terms of tensile, compression and shear (V-notched rail shear, VNRS) experiments. The specimen dimensions for the specific test case can be found in the appropriate standards [3-5]. For the case of tensile and compression loading strain gauges are applied to both sides of the specimens to monitor superposed bending. Most of the specimens exhibit bending strains below 5 %. The few specimens showing higher bending strains are not considered in the calculation of the material properties. The VNRS experiments are accompanied by digital image correlation (DIC) for strain measurement. Furthermore, the coefficients of thermal expansion (CTE) are determined by dilatometer measurements with a heating rate of $1\ \mathrm{K/min}$ of 20 specimens parallel and perpendicular to the fibre direction, respectively. The glass transition temperature T_g is determined by differential scanning calorimetry (DSC) measurements from three specimens randomly taken from composite plates. The final results of the material characterisation as well as the nominal ply thickness are given in table **1**.

Table 1: Material properties of T700SC/LY556 carbon composite UD-ply

E_{11} [GPa]	E_{22}/E_{33} [GPa]	G_{12}/G_{13} [GPa]	G_{23}^{*} [GPa]	ν_{12}/ν_{13} [−]	ν_{23}^{**} [−]
129.4 ± 5.4	8.05 ±0.44	3.92 ± 0.19	2.85 ± 0.15	0.317 ± 0.007	0.41

$R_{\parallel}^{+}$ [MPa]	$R_{\perp}^{+}$ [MPa]	$R_{\parallel}^{-}$ [MPa]	$R_{\perp}^{-}$ [MPa]	$R_{\parallel\perp}$ [MPa]
2089 ± 53	36.2 ± 5.3	1032 ± 221	164.4 ±7.9	52.2 ± 5.4

$\alpha_{\parallel}^{***}$ [10^{-6}/K]	$\alpha_{\perp}^{***}$ [10^{-6}/K]	T_g [°C]	t_{nom}^{*} [mm]
0.5	38	146.4 ± 2.4	0.181

* calculated, ** assumed , *** at room temperature

A FE-model of the specimen is further on used to calculate the residual stresses. The complex shrinking behaviour of matrix and fibre during the multistage fabrication regime is simplified to a linear thermal analysis with the given material properties of table 1 and calibrated by measurements of the residual crack opening (COD) and residual deformations. Details about that methodology are currently published elsewhere. As a result the residual stress state of the specimen can be modelled by using a temperature step $\Delta T = -110\ \mathrm{K}$ leading to a homogeneous stress field in the 90°-layer of $\sigma_{res,1}^{90} = -15.9\ \mathrm{MPa}$; $\sigma_{res,2}^{90} = 25.7\ \mathrm{MPa}$ and the 0°-layer of $\sigma_{res,1}^{0} = -43.2\ \mathrm{MPa}$; $\sigma_{res,2}^{0} = 26.9\ \mathrm{MPa}$.

3 Local in situ strain measurement of cracked laminates at tension and compression

3.1 Methodology

In a second step, another cross-ply specimen is first loaded in quasi-static tension to introduce several off-axis cracks in the 90°-ply and afterwards cyclically loaded for one cycle with different load ratios in the range of $R_{glob} = \{0;\ -1;\ -2.66\}$. The laminate strain is measured by an extensometer with 50 mm gauge length on a ZWICK 1465 universal testing machine equipped with a 50 kN load cell. Additionally, the local strain distribution has been measured by use of an ARAMIS 5M DIC system. However, due to limitations of the test setup, the local strain measurement is performed in 2D only. All the experiments are performed with an anti-buckling device attached to the specimen to prevent unpreferable specimen buckling when loaded in compression. To enhance the comparability between the tests with different load ratios, all test are performed with the anti-buckling device, even if it is not necessary, e.g. in the tensile tests.

3.2 Results

The first quasi-static load step is conducted with a cross head speed of 1 mm/min up to a maximum force of 16.8 kN, which leads to a maximum nominal laminate stress of $\sigma_{max}^{lam} = 322\ \mathrm{MPa}$. Throughout the experiment, several cracks occurred within the observed area, consecutively. The laminate stress-strain curve as well as the observations of the cracking state at different load levels is depicted in figure 2. It can clearly be seen, that the increasing damage within the 90°-ply leads to non-linear stress-strain behaviour of the laminate. First cracks occurred at laminate strain levels of about $\varepsilon_{ini} \approx 0.27\ \%$, which is recognized as a slight divergence between the experimental stress-strain behaviour and the linear elastic material behaviour calculated by use of the initial stiffness. All the cracks within the area of observation initiated at different macroscopic load levels and they span the entire transverse ply thickness. However, some cracks incline an angle different from 90° with the direction of loading, indicating shear or compression failure. It is not fully understood, why the cracks are not perpendicular to the load direction, but it is assumed that the pretension of the anti-buckling device in thickness direction introduces irregular transverse compression loads and therefore changes the mode of fracture. This issue is subject to further investigation and will be clarified.

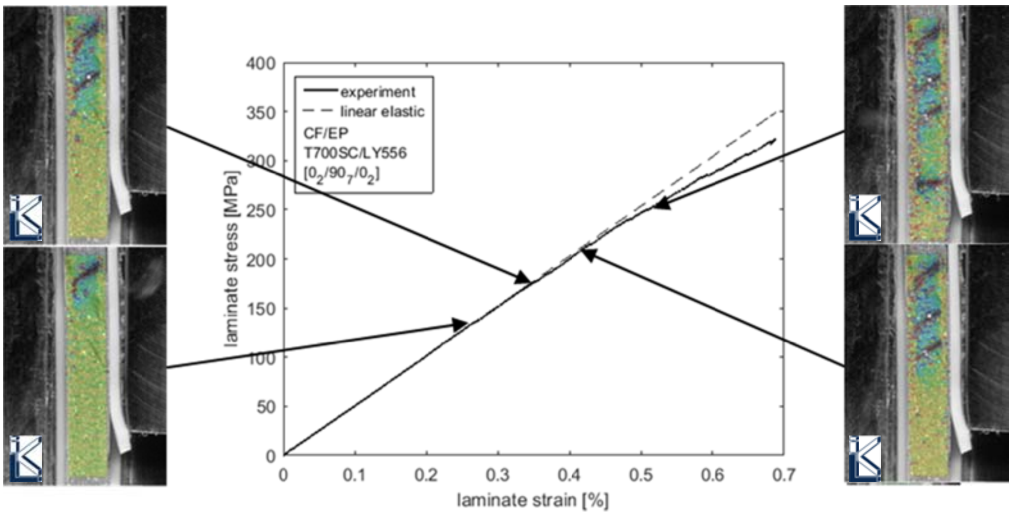

Figure 2: Experimentally determined stress-strain relation of cross-ply laminate subjected to axial tensile loading and corresponding cracking state of the 90°-ply within the area of observation.

To compare the global laminate response with the local material response it is useful to take the local strains averaged over the observation area into account. As seen from figure 3, the global and local stress strain response is in good agreement at the beginning of the test, when no cracks can be observed. At a laminate stress of $\sigma_{max}^{lam} = 132\ \mathrm{MPa}$ the first microcrack in the observed area formed, leading to a significant drop of the averaged local strain from $\varepsilon_{loc} = 0.27\ \%$ to $\varepsilon_{loc} = 0.19\ \%$. Although the local strain data is a little noisy

after initiation of the first crack (due to a change of the sprayed paint pattern), it is clearly seen that with further increase of external load the local averaged strain rises again up to approximately the same value of $\varepsilon_{loc} = 0.27\ \%$ before the next crack forms. This behaviour can be observed repeatedly for all the cracks in the observed area, indicating a constant crack initiation strain or a constant strain energy release rate.
However, due to the calibration of the DIC system to a reference stage at the beginning of the test, only mechanical strains applied by external loads can be measured. The residual strains in the laminate cannot be respected in terms of optical strain measurement.
As discussed in section 2 there are significant residual stresses within the cross-ply after curing due to the different fibre angles. This is important when conducting fatigue experiments with load ratios that are generally applied in terms of global laminate load ratios.

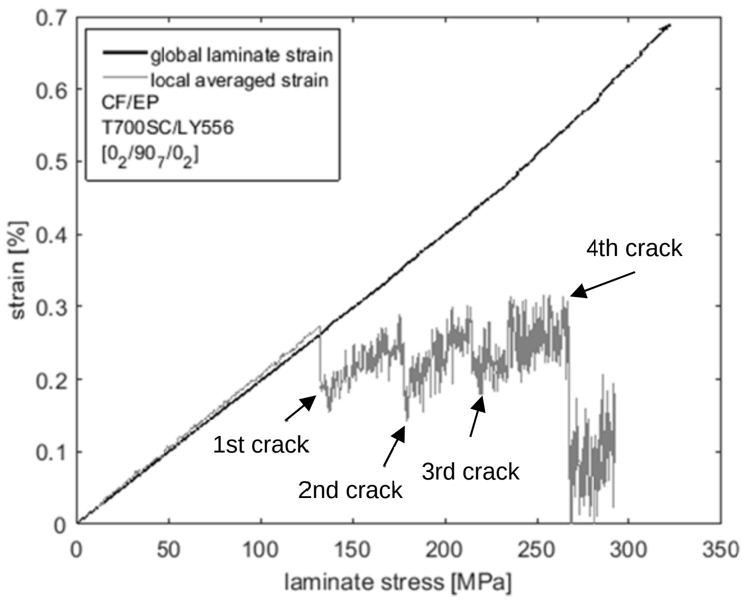

Figure 3: Experimentally determined global and local strain-stress relation of a CF/EP cross-ply laminate containing several transverse cracks.

For the laminate used in this study, the residual stresses in the 90°-ply have been calculated in section 3 to $\sigma_{res}^{90} = [-15.9,\ 25.7,\ 0.0]^{\mathrm{T}}\ \mathrm{MPa}$. For the tested load ratios of $R_{glob} = \{0;\ -1;\ -2.66\}$ the local load ratio in the 90°-ply can be calculated by considering the residual stresses as a shift of the mean stress. The local 90°-ply stress ratio in transverse direction for the uncracked laminate can be calculated as follows

$$R_{loc} = \frac{\sigma_{min}}{\sigma_{max}} = \frac{(\sigma_m^{90} + \sigma_{res}^{90}) - \sigma_a^{90}}{(\sigma_m^{90} + \sigma_{res}^{90}) + \sigma_a^{90}}. \tag{1}$$

Additionally, the load ratio is calculated for the areas between the 90°-ply cracks as depicted in figure 4. The results are plotted against the globally applied load ratio.

As seen from figure 4 local load ratio determined from the local averaged strains between two adjacent cracks is close to the globally applied load ratio. This is, as mentioned before, due to the missing information of the residual stresses and strains within the 90°-ply. It should be highlighted that the deviation from the applied load ratio is the highest for crack interval 4-5, which has a nearly perpendicular crack alignment.

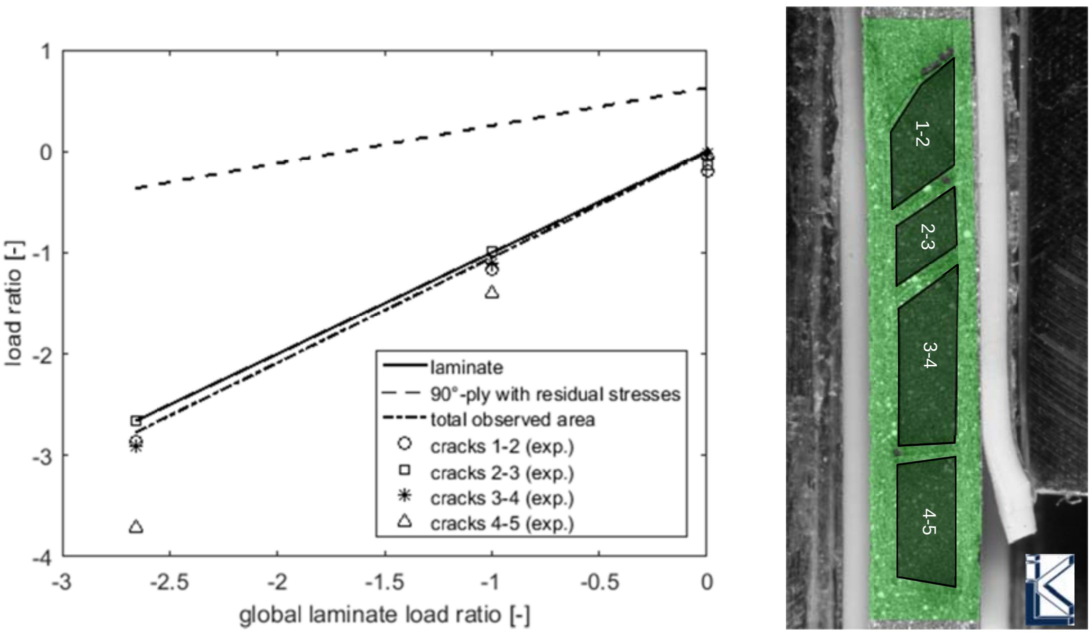

Figure 4: Calculated load ratios for the uncracked laminate and 90°-ply with local load ratios between cracks 1-5 measured by digital image correlation. Note that the DIC cannot determine residual stresses within the observed area due to calibration at a mechanically unloaded reference stage.

From section 2 it came clear, that the cracks in the off-axis ply remain opened even if the laminate is unloaded and unmounted from the testing machine. It is therefore of interest, whether these cracks close under compression loading. The single cycle tests for $R_{glob} = \{0;\ -1;\ -2.66\}$ with a maximum stress level of $\sigma_{max}^{lam} = 95\ \mathrm{MPa}$ are also accompanied by DIC measurements. The corresponding stress-strain relations of the area between cracks 3 - 4 and 4 - 5 and the overall laminate stress-strain relations for the laminate are given in figure 5. Please note, that for reasons of clarity only the unloading paths are shown here. It can be seen that in all cases the local strain within the 90°-ply is significantly lower than the global laminate strain due to the existence of microcracks. At the crack locations the load transfer between the plies is prevented and the 90°-ply starts carrying load again in some distance from the crack, which is called crack shielding. Further, the local averaged strain between the cracks also depends on the crack distance, as expected [6-8]. It is further assumed that the change of the local ply strain state is only altered by the formation of cracks. Potential influences of material nonlinearity and delaminations are neglected at this point. The averaged crack opening displacement $\tilde{u}_{COD}$ can therefore be written as the result of the averaged change of ply strain $\Delta\varepsilon^{90}$ in the direction of loading within a cracked unit cell of length L

$$\tilde{u}_{COD} = \Delta\varepsilon^{90} L = (\varepsilon^{lam} - \varepsilon^{90}) L. \quad (2)$$

The COD calculations have been carried out for two cracking intervals (3-4 and 4-5) by use of the stress-strain relations in figure 5. For simplification it is assumed that the cracks are perpendicular to the axial laminate direction although they are not perfectly aligned.

For $\boldsymbol{R_{glob}} = \mathbf{0}$ (tension-tension) the global laminate strain as well as the local averaged strain follows linear trends with increasing load. It can further be seen, that the local averaged strain in the smaller crack interval L_{45} is significantly smaller than in the larger interval L_{34}. The difference between the two cracked areas at maximum tension load is about $\Delta\varepsilon = 0.05$ %. Considering the corresponding CODs, it is clearly shown that they follow a linear trend and are increasing with higher loads, as seen in figure 5a. This has also been found by VARNA ET AL. [8] for GF/EP cross-ply laminates with varying 90°-ply thickness.
However, when the loading direction is reversed into compression loading non-linear behaviour can be observed showing a progressive trend, figure 5b. In case of $\boldsymbol{R_{glob}} = -\mathbf{1}$ the nonlinearity of the stress-strain curve is only small when the specimen is loaded in compression. This becomes clearer by consideration of the calculated corresponding COD vs. load level. While loaded in tension, the CODs follow a linear trend in the same way as for load ratio $R_{glob} = 0$, but the slope changes with ongoing unloading into compression loads. The polynomial fits of the CODs show a declining behaviour, which can be interpreted as a consecutively closing of the crack faces.
For stress ratio $\boldsymbol{R_{glob}} = -\mathbf{2.66}$ the nonlinear behaviour enhances with further compression loading, as seen in figure 5c. It is interesting to note, that with increasing compression loading, the stiffness should increase, indicating that more load is carried by the cracked areas. If the cracks would close completely, the initial stiffness should be reached. But due to the dominating nonlinear behaviour of the 0°-layer these effects are shielded here. Taking the corresponding CODs the hypotheses holds true and the declining behaviour under compression loading is pronounced. Although the stress-strain curves do not significantly deviate from each other, the difference of the COD at $\sigma_c^{lam} = -250$ MPa is obvious and is about $1\ \mu m$. This can be explained by the different lengths of the cracked intervals.

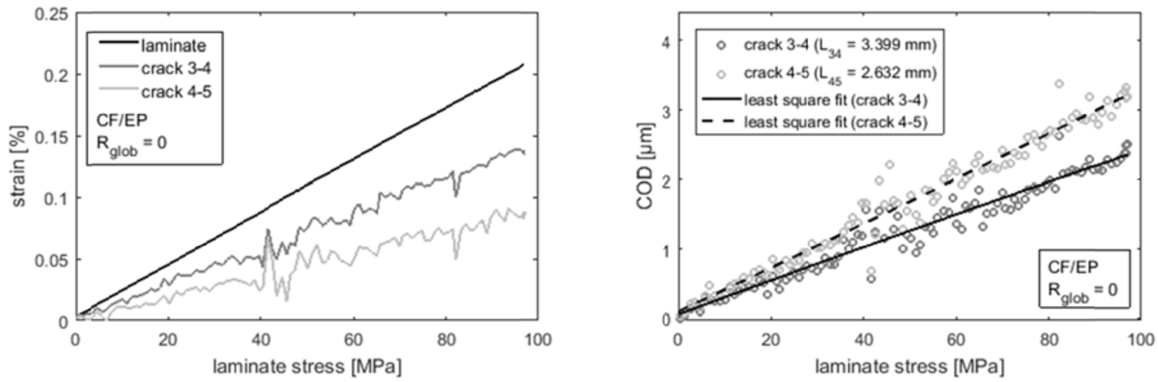

(a)

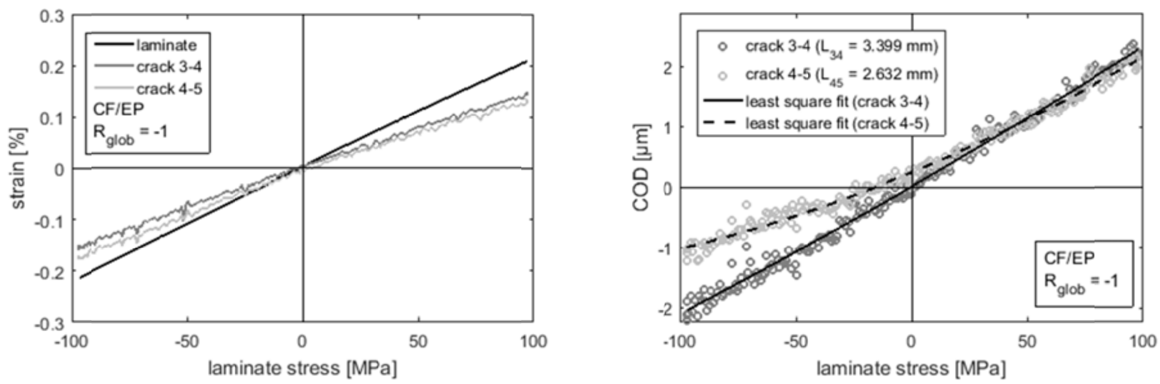

(b)

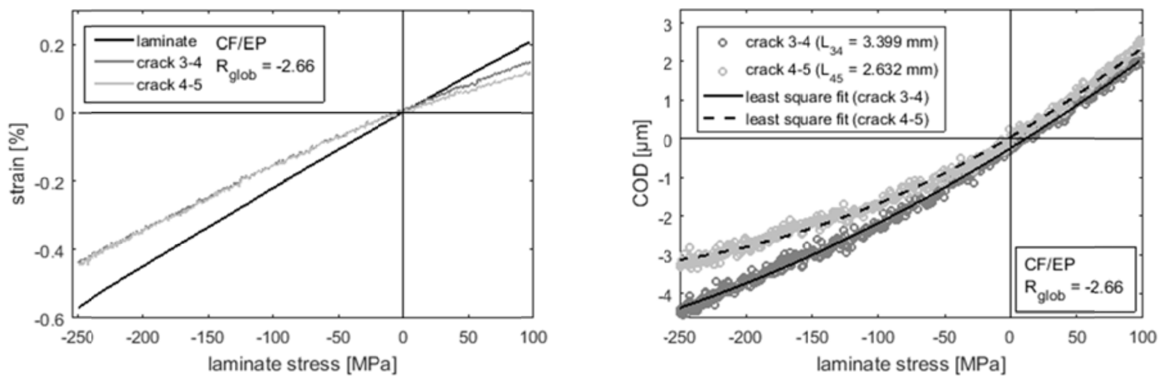

(c)

Figure 5: **Local averaged and global laminate strains vs. laminate stress. The length of the cracking intervals are $L_{34} = 3.399$ mm and $L_{45} = 2.632$ mm. Crack opening displacement (COD) calculated from local averaged strains for different load ratios. Polynomial least square fits of crack opening displacements are of order 2.**

4 Discussion of results

The results presented in section 3 are highlighting the influence of microcracks in off-axis plies on the local stress-strain fields. It is clearly shown, that cracks disturb the load transfer into the 90°-ply and reduce the stresses and strains in their vicinity. Further it was pointed out that the linear dependency of the CODs on the applied load is not valid in case of compression loading. From figure 5 it is seen, that negative crack opening displacements are calculated in case of compression loading, which would actually mean that the crack faces intersect and is not reasonable from a physical point of view. But, keeping in mind that DIC only measures the mechanically applied strains and that due to residual stresses a residual crack opening remains it is concluded, that the cracks close partially under compression loading, leading to gradually increasing load carrying capability of the cracked 90°-ply. It can be argued, that the total load carrying capability of the cracked ply should be restored, when the cracks close completely. This results in identical slopes of the laminate stress-strain relations for global and local measurements. However, this behaviour was not observed even for higher compression loads of $\sigma_c^{lam} = -250\ \mathrm{MPa}$, indicating that the cracks are not fully closed. This finding is supported by the calculation of the local CODs of two cracked intervals between cracks 3-4 and 4-5.

From the previous findings it can be concluded, that due to crack closure at high compression loads, load transfer over crack faces is possible again. Therefore the compression YOUNG's and shear modulus are restored in parts leading to different stress-strain relations under tension and compression loading, respectively. Further the question arises if combined compression-shear loadings have a severe impact on laminate damage. This point gains even more importance for off-axis angles different from 90° were mode II crack growth is also possible under compression loads.

5 Conclusion

The experimental investigation of the cracking behaviour of T700S/LY556 carbon fibre-epoxy laminates has shown the importance of residual stresses on crack closure and fatigue behaviour. The main findings of the study are summarised in the following.

Residual stresses change the load ratio of uncracked off-axis plies what can be interpreted as a shift of the mean stress by the amount of the residual stress. It is therefore interesting to note, that from a ply-wise point of view, each ply exhibits different load-ratios during fatigue loading.

It was found from local DIC measurements that the COD is linearly related to the applied load in case of tension loading. When the load is reversed, the stress-strain relation reveals nonlinear behaviour, which is addressed to partial closing of the corresponding cracks. The crack closing increases with higher compression loads, but the cracks do not close completely up to a compression load of $\sigma_c^{lam} = -250\ \mathrm{MPa}$.

Acknowledgements

The authors specifically acknowledge the funding of this work by the German research foundation (DFG) within the Project GU 614/10-1 and our scientific partners at Polymer Composites (TU Hamburg-Harburg), IKV at RWTH Aachen and ISD (Leibniz Universität Hannover).

References

[1] Gude, M.; Hufenbach, W.; Kirvel, Ch.: Time and temperature dependence on the snap-through behaviour of adaptive bistable composites, International Conference on Composite Materials 2013 (ICCM-19) Montreal, Quebec, Canada 28 July - 2 August 2013

[2] Shokrieh, M. (Ed.): Residual Stresses in Composite Materials; Woodhead publishing, ISBN: 978-0-85709-270-0, 2014

[3] ASTM D 7078 - Standard Test Method for Shear Properties of Composite Materials by V-Notched Rail Shear Method

[4] DIN 527 - Kunststoffe - Bestimmung der Zugeigenschaften

[5] DIN 14126 - Bestimmung der Druckeigenschaften in der Laminatebene

[6] Hashin, Z.: Analysis of cracked laminates: a variational approach. Mechanics of materials 4, pp. 121–136, 1985

[7] Lundmark, P.; Varna, J.: Constitutive Relationships for Laminates with Ply Cracks in In-plane Loading. International Journal of Damage Mechanics 14, pp. 235–259, 2005, doi:10.1177/1056789505050355

[8] Varna, J.; Berglund, L.A.; Talreja, R.; Jakovics, A.: A study of the opening displacement of transverse cracks in cross-ply laminates. International Journal of Damage Mechanics 2, pp. 272–289, 1993